

Sliding Mode Control for Uncertain Thermal SOFC Models with Physical Actuator Constraints

SCAN 2012: 15th GAMM-IMACS Intl. Symposium on Scientific
Computing, Computer Arithmetic and Verified Numerical
Computations

Novosibirsk, Russia

September 27, 2012

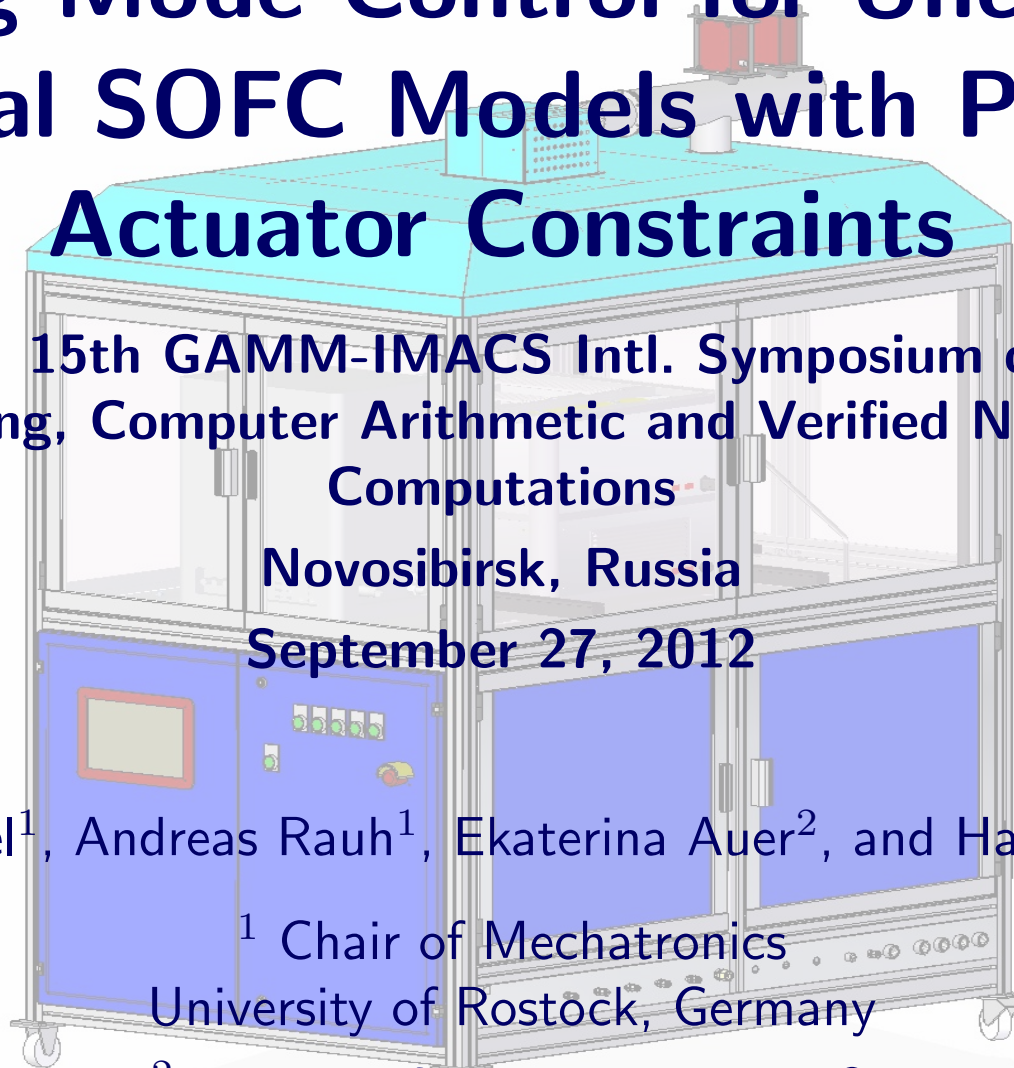
Thomas Dötschel¹, Andreas Rauh¹, Ekaterina Auer², and Harald Aschemann¹

¹ Chair of Mechatronics

University of Rostock, Germany

² Faculty of Engineering, INKO

University of Duisburg-Essen, Germany

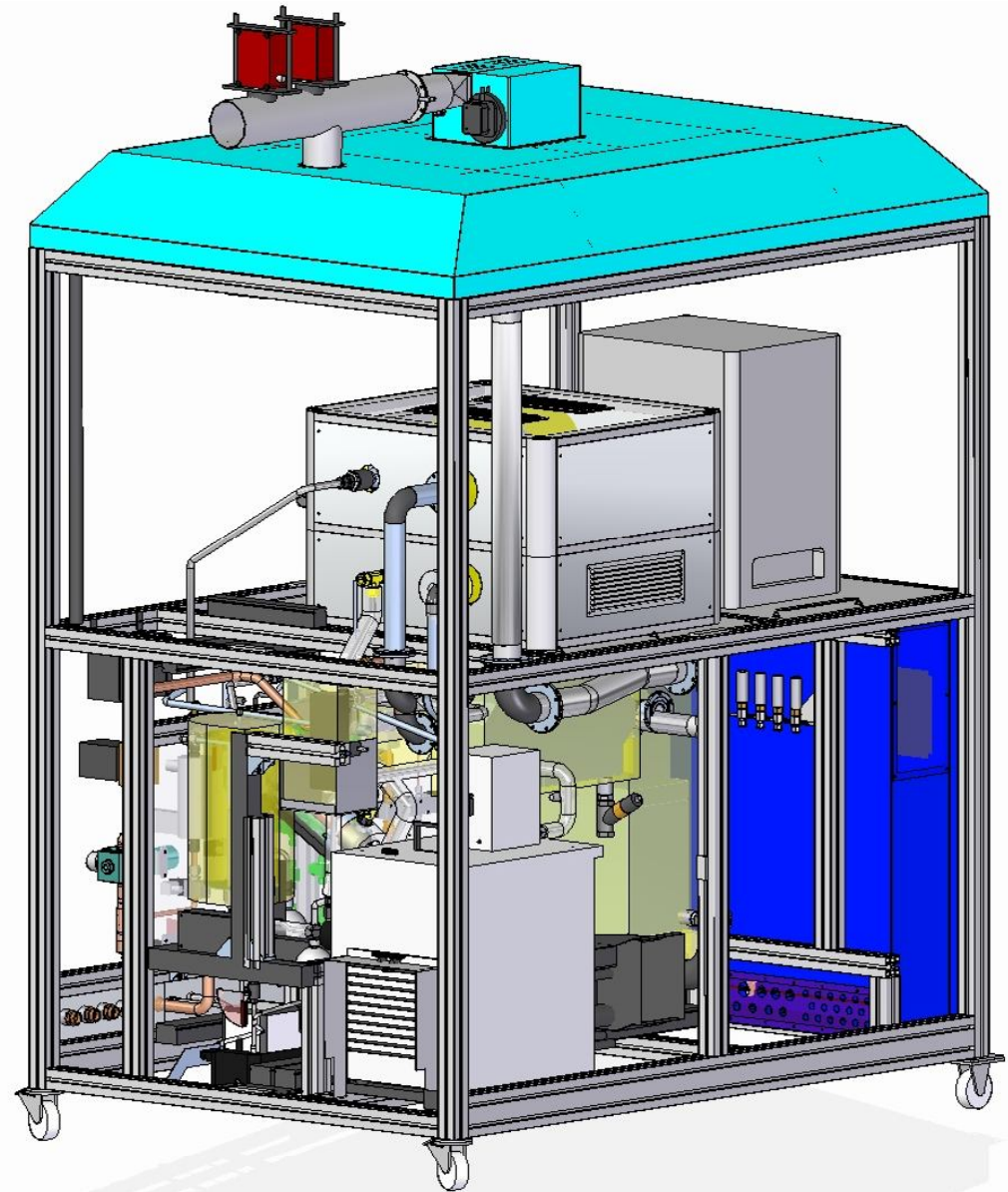


Contents

- Working principles of Solid Oxide Fuel Cell (SOFC) systems
- Thermal modeling of SOFC stack modules
- Physical actuator constraints in SOFC systems
- Design of robust sliding mode control strategies
- Numerical validation and verification
- Conclusions and outlook

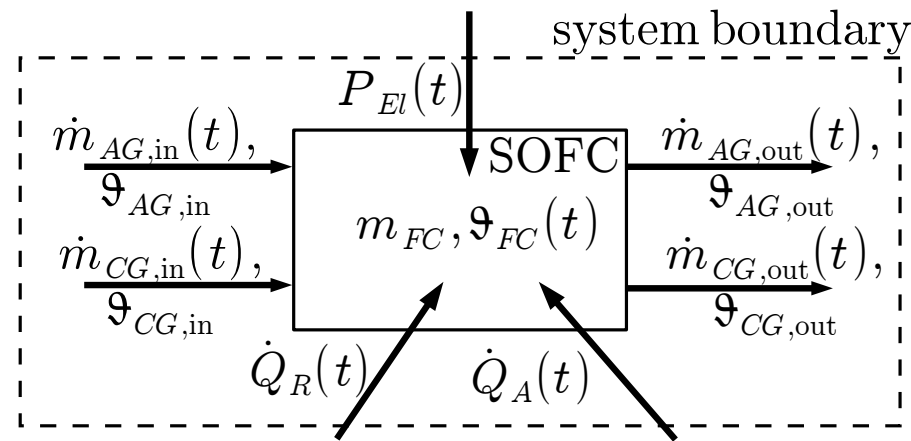
Working principles

- Fluid supply (fuel gas, air)
- Independent preheaters for fuel gas and air
- Stack module containing fuel cells in electric series connection
- Variable electric load as a disturbance



Modeling Approach

Energy balance of the SOFC stack module



- Control-oriented modeling of a SOFC stack module for the derivation of control and observer strategies
- Integral balancing of a non-stationary energy conversion process in the whole stack module as well as in individual finite volume elements
- Impact of the variation of the internal energy on the local temperature distribution in the stack module



Modeling Approach

- Relation between the variation of the internal energy and the stack temperature for constant material parameters c_{FC} and m_{FC}

$$\frac{dE_{FC}(t)}{dt} = c_{FC} \cdot m_{FC} \cdot \frac{d\vartheta_{FC}(t)}{dt}$$

- Modeling of the effects on the internal energy

$$\begin{aligned} \frac{dE_{FC}(t)}{dt} = & C_{AG}(\vartheta_{FC}, t) (\vartheta_{AG,in}(t) - \vartheta_{FC}(t)) \\ & + C_{CG}(\vartheta_{FC}, t) (\vartheta_{CG,in}(t) - \vartheta_{FC}(t)) \\ & + \dot{Q}_R(t) + P_{El}(t) + \dot{Q}_A(t) \end{aligned}$$

- Reaction heat flow of the hydrogen oxidation reaction

$$\dot{Q}_R = \frac{\Delta_R H(\vartheta_{FC}) \cdot \dot{m}_{H_2}(t)}{M_{H_2}}$$

Modeling Approach

- Relation between the variation of the internal energy and the stack temperature for constant material parameters c_{FC} and m_{FC}

$$\begin{aligned} c_{FC} \cdot m_{FC} \cdot \frac{d\vartheta_{FC}(t)}{dt} = & C_{AG}(\vartheta_{FC}, t) (\vartheta_{AG,in}(t) - \vartheta_{FC}(t)) \\ & + C_{CG}(\vartheta_{FC}, t) (\vartheta_{CG,in}(t) - \vartheta_{FC}(t)) \\ & + \dot{Q}_R(t) + P_{El}(t) + \dot{Q}_A(t) \end{aligned}$$

- Heat transfer including a linearized model for the heat radiation to the ambient media

$$\dot{Q}_A = \frac{1}{R_A} (\vartheta_A - \vartheta_{FC})$$

- Ohmic loss effects in the stack material

$$P_{El}(t) = R_{El} I^2(t)$$

Modeling Approach

- Relation between the variation of the internal energy and the stack temperature for constant material parameters c_{FC} and m_{FC}

$$\begin{aligned}
 c_{FC} \cdot m_{FC} \cdot \frac{d\vartheta_{FC}(t)}{dt} = & C_{AG}(\vartheta_{FC}, t) (\vartheta_{AG,in}(t) - \vartheta_{FC}(t)) \\
 & + C_{CG}(\vartheta_{FC}, t) (\vartheta_{CG,in}(t) - \vartheta_{FC}(t)) \\
 & + \dot{Q}_R(t) + P_{El}(t) + \dot{Q}_A(t)
 \end{aligned}$$

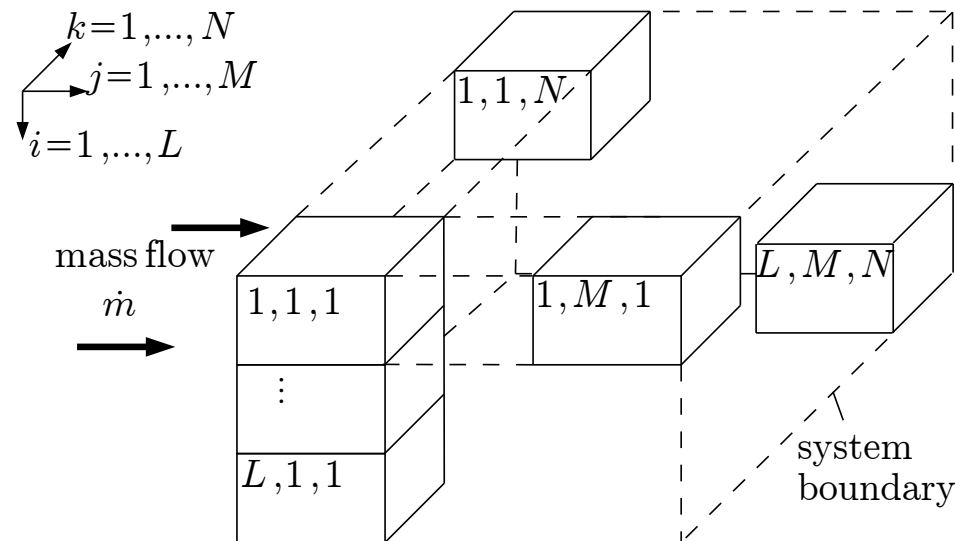
- Anode gas: Heat capacity approximated by 2nd-order polynomials for c_χ with $\chi \in \{H_2, N_2, H_2O\}$

$$\begin{aligned}
 C_{AG}(\vartheta_{FC}, t) = & c_{H_2}(\vartheta_{FC}) \dot{m}_{H_2}(t) \\
 & + c_{N_2}(\vartheta_{FC}) \dot{m}_{N_2}(t) + c_{H_2O}(\vartheta_{FC}) \dot{m}_{H_2O}(t)
 \end{aligned}$$

- Cathode gas: Heat capacity approximated with 2nd-order polynomials for c_{CG}

$$C_{CG}(\vartheta_{FC}, t) = c_{CG}(\vartheta_{FC}) \cdot \dot{m}_{CG}(t)$$

Semi-Discretization: The Finite Volume Method



- Semi-discretization into $n_x = L \cdot M \cdot N$ finite volume elements to describe the internal temperature distributions
- Local energy balances lead to a set of n_x coupled ODEs represented by a state vector $x^T = [\vartheta_{1,1,1}, \dots, \vartheta_{L,M,N}] \in \mathbb{R}^{n_x}$
- System boundary includes the thermal stack insulation



Semi-Discretization: The Finite Volume Method

- ODE for the local temperature distribution in a SOFC stack module

$$\begin{aligned}
 c_{i,j,k} \cdot m_{i,j,k} \cdot \dot{\vartheta}_{i,j,k}(t) &= C_{AG,i,j,k}(\vartheta_{i,j,k}, t) \left(\vartheta_{i,j-1,k}(t) - \vartheta_{i,j,k}(t) \right) \\
 &\quad + C_{CG,i,j,k}(\vartheta_{i,j,k}, t) \left(\vartheta_{i,j-1,k}(t) - \vartheta_{i,j,k}(t) \right) \\
 &\quad + \dot{Q}_{\eta,i,j,k}(t) + \dot{Q}_{R,i,j,k}(t) + P_{El,i,j,k}(t)
 \end{aligned}$$

- Modeling of local temperature-dependent and time-varying influence factors

Heat flow:
$$\dot{Q}_{\eta,i,j,k}(t) = \sum_{\eta \in \mathcal{N}} \frac{1}{R_{th,\eta}^{i,j,k}} (\vartheta_{\eta}(t) - \vartheta_{i,j,k}(t))$$

Reaction heat flow:
$$\dot{Q}_{R,i,j,k}(t) = \frac{\Delta_{RH_{i,j,k}}(\vartheta_{i,j,k}) \cdot \dot{m}_{H_2,i,j,k}(t)}{M_{H_2}}$$

Ohmic losses:
$$P_{El,i,j,k}(t) = R_{El,i,j,k} I_{i,j,k}^2(t)$$

Semi-Discretization: The Finite Volume Method

Case 1: Semi-discretization into a single finite volume element leads to the global energy balance described before

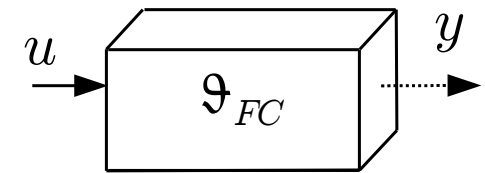
- State variable x and output variable y

$$x(t) = \vartheta_{FC}(t)$$

$$y(t) = h(x) = \vartheta_{FC}(t)$$

- Nonlinear ordinary differential equation

$$\dot{\vartheta}_{FC} = \Phi(\vartheta_{FC}(t), u(t))$$



Case 2: Semi-discretization into three finite volume elements oriented in the direction of mass flow

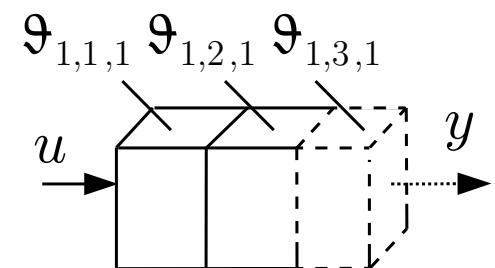
- State vector x and output variable y

$$x(t) = [\vartheta_{1,1,1}(t), \vartheta_{1,2,1}(t), \vartheta_{1,3,1}(t)]^T$$

$$y(t) = h(x) = \vartheta_{1,3,1}(t)$$

- Set of coupled nonlinear ordinary differential equations

$$\dot{x}(t) = \Phi(x(t), u(t))$$



State Equations — Reformulation for Control Synthesis

- Input-affine description of the nonlinear thermal subsystem

$$\dot{x}(t) = f(x(t)) + g(x(t)) \cdot u(t), \quad x \in \mathbb{R}^{n_x}$$

$$y(t) = h(x(t)), \quad y \in \mathbb{R}^{n_y}$$

$$u(t) = \dot{m}_{CG}(t) \cdot \Delta\vartheta(t)$$

- Underlying controller for the preheating device to achieve the temperature difference $\Delta\vartheta$ in the control input $u(t)$

$$\Delta\vartheta(t) := \begin{cases} \vartheta_{CG}(t) - \vartheta_{FC}(t) & \text{for } x(t) = \vartheta_{FC}(t) \\ \vartheta_{CG}(t) - \vartheta_{1,1,1}(t) & \text{for } x(t) = [\vartheta_{1,1,1}(t), \vartheta_{1,2,1}(t), \vartheta_{1,3,1}(t)]^T \end{cases}$$

- Exact input-output linearization with relative degree δ (Computation of the Lie-Derivatives of y)

$$\frac{d^i y}{dt^i} = L_f^i h(x) = L_f \left(L_f^{i-1} h(x) \right), \quad i = 0, \dots, \delta - 1$$

- Relative degree δ denotes the smallest order explicitly depending on the input u

Modeling Approach — Transformation of the State-Space

- Nonlinear transformation of the state equations with the relative degree $\delta = n_x$ according to

$$z^T = [z_1 \ z_2 \ z_3] = [y \ \dot{y} \ \ddot{y}] = [h(x) \ L_f h(x) \ L_f^2 h(x)]$$

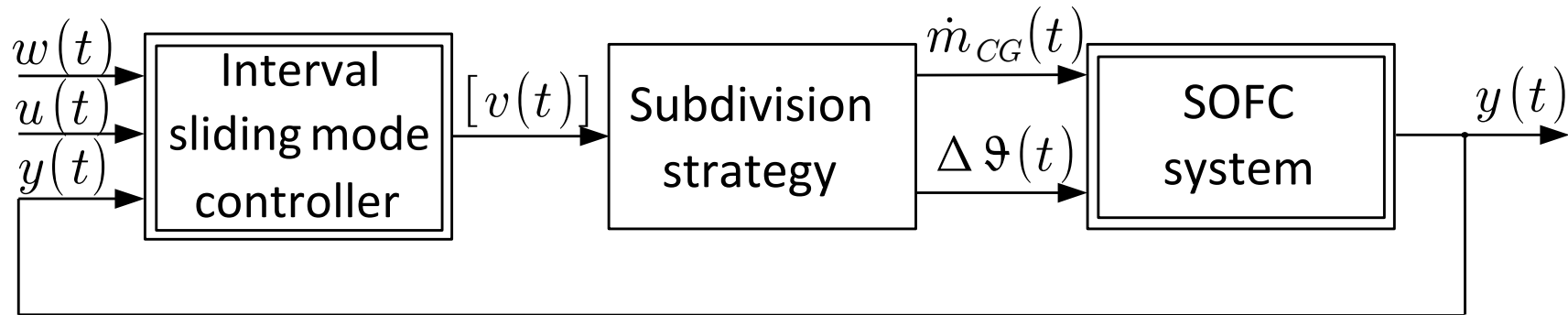
- Nonlinear controller normal form (NCNF)

$$\dot{z} = \begin{bmatrix} \dot{z}_1 \\ \dot{z}_2 \\ \dot{z}_3 \end{bmatrix} = \begin{bmatrix} L_f h(x) \\ L_f^2 h(x) \\ L_f^3 h(x) \end{bmatrix} + \begin{bmatrix} 0 \\ 0 \\ L_g L_f^2 h(x) \end{bmatrix} u$$

- Feedback linearizing control law for sufficiently small variations of the mass flow used for the heat-up phase of the SOFC

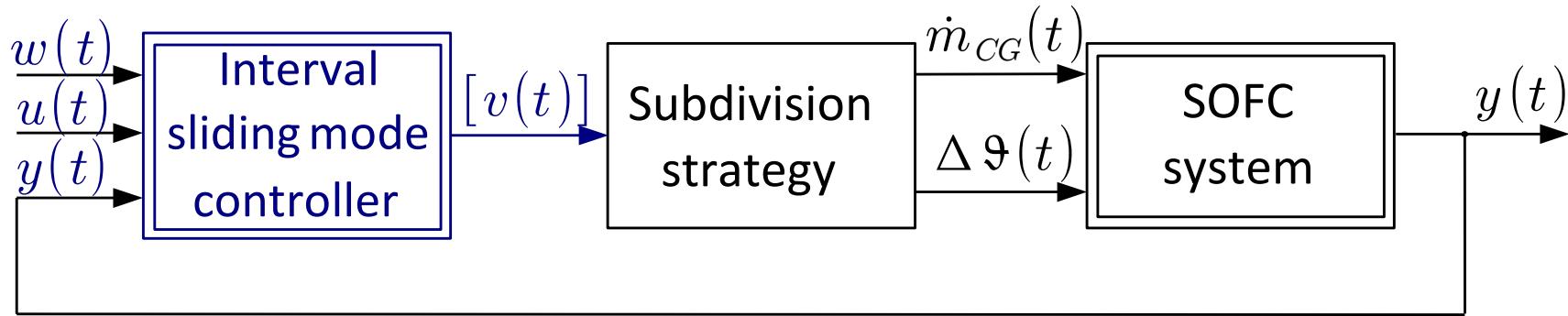
$$u := \frac{-L_f^3 h(x) - \alpha_0 h(x) - \alpha_1 L_f h(x) - \alpha_2 L_f^2 h(x) + \mu(t)}{L_g L_f^2 h(x)}$$

Robust Sliding Mode Control



- Rejection of disturbances in the neighborhood of a desired operating point by means of sliding mode control accounting for physical actuator constraints
- Online application of interval analysis to handle uncertainty in measurements as well as state reconstruction errors
- Minimization of a quality criterion for choosing adequate values for \dot{m}_{CG} and $\Delta\vartheta$ to manipulate the enthalpy flow of the cathode gas
- Online subdivision strategy allows for converting the interval-based controller output $[v(t)]$ into a point-valued system input $u(t) = \dot{m}_{CG}(t) \cdot \Delta\vartheta(t)$
- Guarantee of asymptotic stability in spite of uncertainty

Robust Sliding Mode Control



- Mathematical model of the SOFC system in an input-affine description is extended by a bounded disturbance $d \in [d]$

$$\begin{bmatrix} \dot{z}_1 \\ \dot{z}_2 \\ \dot{z}_3 \end{bmatrix} = \begin{bmatrix} z_2 \\ z_3 \\ \tilde{a}(z, p, d) \end{bmatrix} + \begin{bmatrix} 0 \\ 0 \\ \tilde{b}(z, p) \end{bmatrix} v$$

- Disturbance influences the system according to $\tilde{a} = L_f^3 h + d$
- Interval parameters $p \in [p]$ have been identified offline in a separate work

Robust Sliding Mode Control

- Definition of an asymptotically stable sliding surface $s(\tilde{z}) = 0$ with the tracking error $\tilde{z}_1^{(j)} = z_1^{(j)} - z_{1,d}^{(j)}$

$$s(\tilde{z}) = \tilde{z}_1^{(2)} + \alpha_1 \tilde{z}_1^{(1)} + \alpha_0 \tilde{z}_1^{(0)} = 0$$

and the output z_1 and its time derivatives $z_1^{(j)}$, $j = 1, \dots, \delta - 1 = n_x - 1$

- Stabilization of the motion towards the sliding surface by a suitable Lyapunov function V

$$V = \frac{1}{2}s^2 > 0 \quad \text{for } s \neq 0, \quad \text{and its time derivative } \dot{V} = s\dot{s}$$

- The condition $\dot{V} = s\dot{s} \leq 0$ for the time derivative of the Lyapunov function is fulfilled with

$$s\dot{s} \leq -\eta s \operatorname{sign}\{s\} \quad \text{which is guaranteed for}$$

$$\dot{s} + \eta \cdot \operatorname{sign}\{s\} = -\beta \cdot \operatorname{sign}\{s\}, \quad \eta, \beta > 0$$

- Control input v is obtained from

$$\tilde{a}(z, p, d) + \tilde{b}(z, p)v - z_{1,d}^{(3)} + \alpha_1 \tilde{z}_1^{(2)} + \alpha_0 \tilde{z}_1^{(1)} = -(\beta + \eta) \cdot \operatorname{sign}\{s\}$$

Robust Sliding Mode Control

- Control law for the disturbance rejection in the thermal subsystem

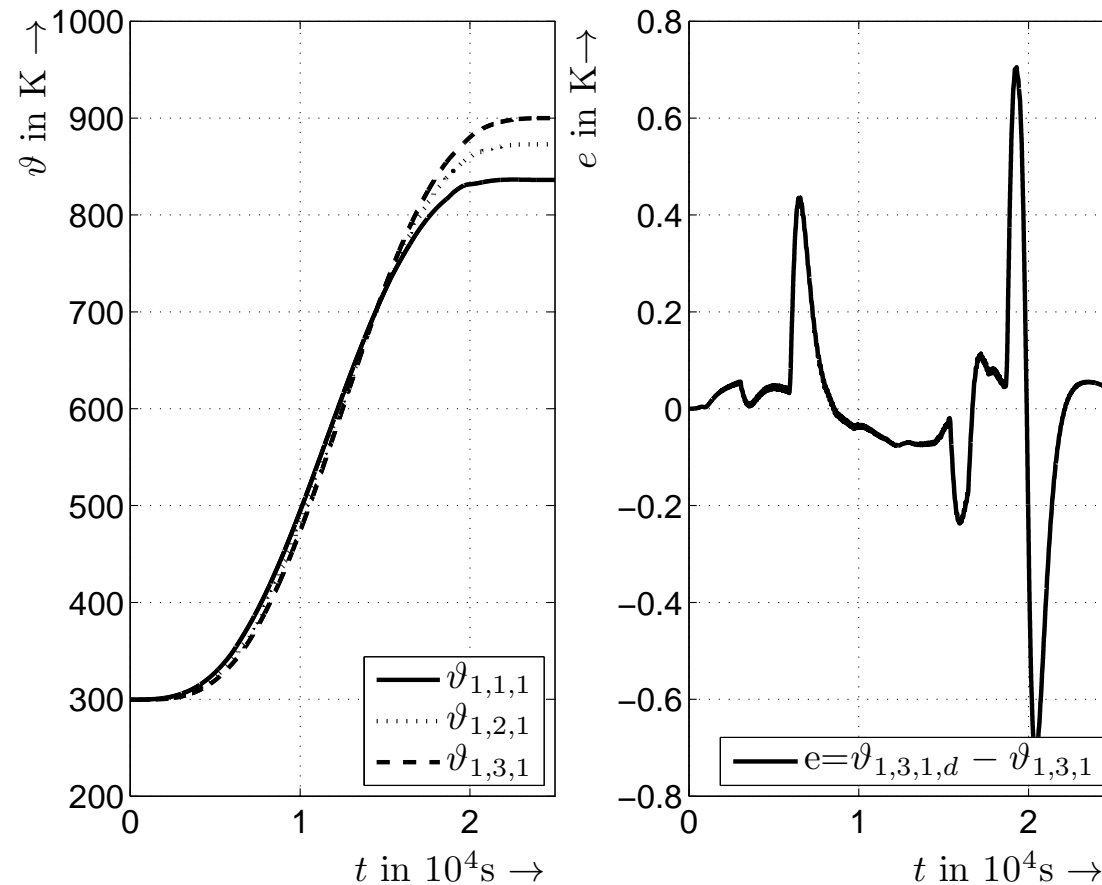
$$[v] := \left[\frac{-\tilde{a}(z, [p], [d]) + z_{1,d}^{(3)} - \alpha_1 \tilde{z}_1^{(2)} - \alpha_0 \tilde{z}_1^{(1)}}{\tilde{b}(z, [p])} - \frac{1}{\tilde{b}(z, [p])} \underbrace{(\eta + \beta)}_{=: \tilde{\eta} > 0} \cdot \text{sign}\{s\} \right] \Bigg|_{\substack{p \in [p] \\ d \in [d]}}$$

- Note: $0 \notin \tilde{b}(z, [p])$ is guaranteed by the physical system properties
- Appropriate choice of the switching amplitude $\tilde{\eta}$ in the case of control design for interval parameters $p \in [p]$ and interval disturbances $d \in [d]$
- Controller output for a guaranteed stabilization of the thermal SOFC system

$$v := \begin{cases} \sup\{[v]\} & \text{for } s \geq 0 \\ \inf\{[v]\} & \text{for } s < 0 \end{cases}$$

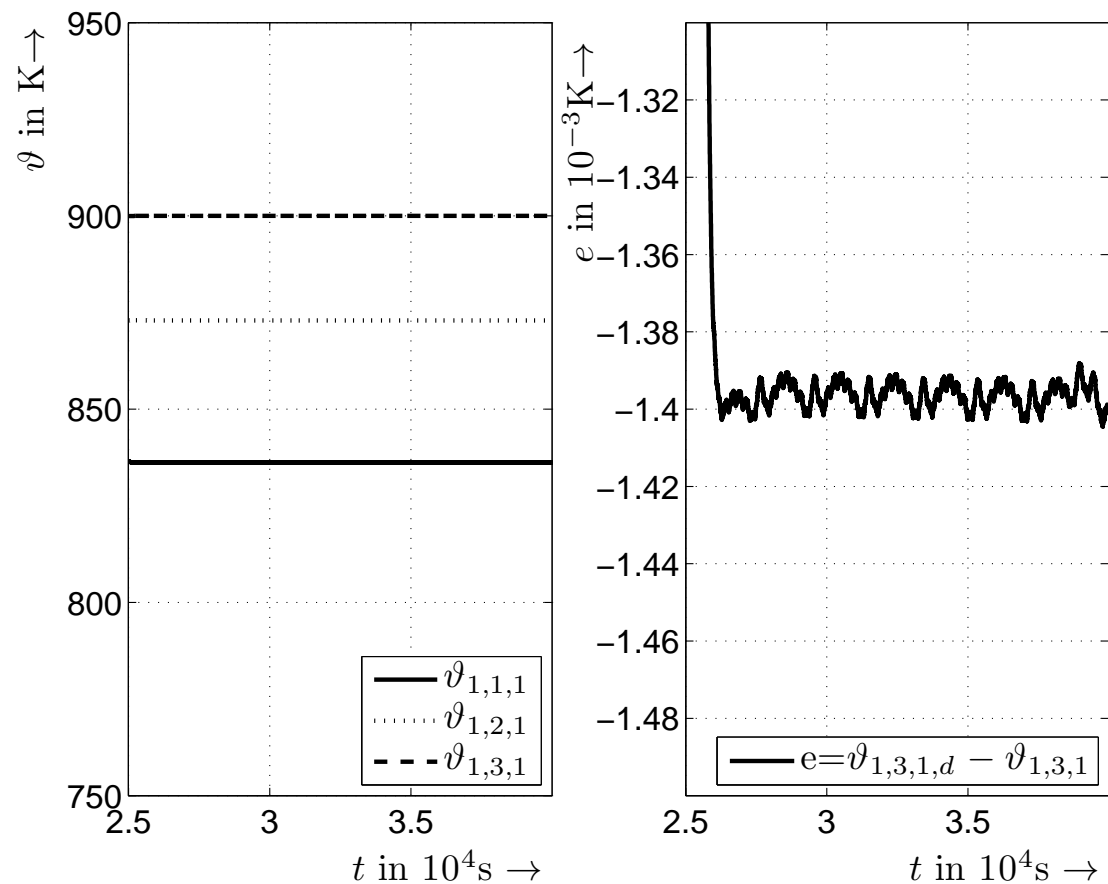
Robust Sliding Mode Control

- Non-stationary heating phase of the SOFC stack module using an exact linearizing control law to reach a desired operating point



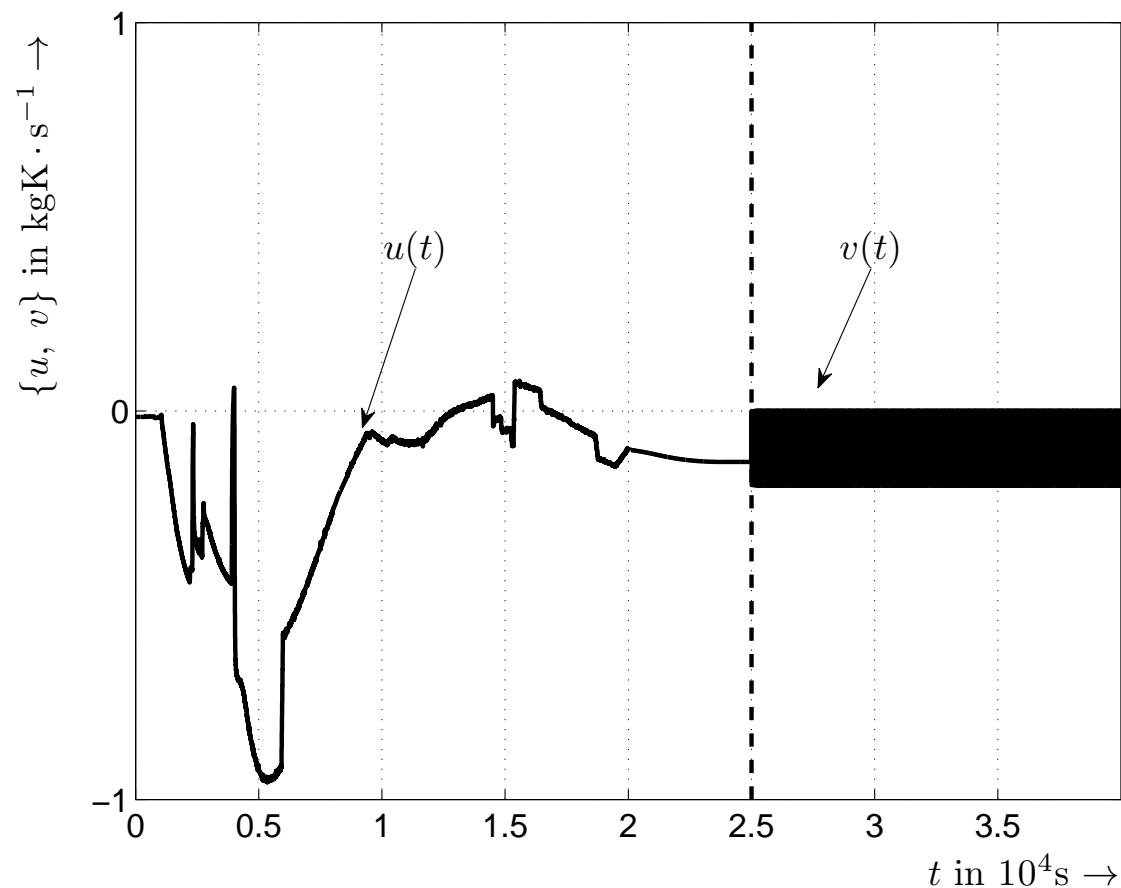
Robust Sliding Mode Control

- Switching to the interval-based sliding mode control law in the point of time $t = 2.5 \cdot 10^4$ s
- **Objective:** Rejection of disturbances and stabilization of desired operating points accounting for bounded state and parameter uncertainty



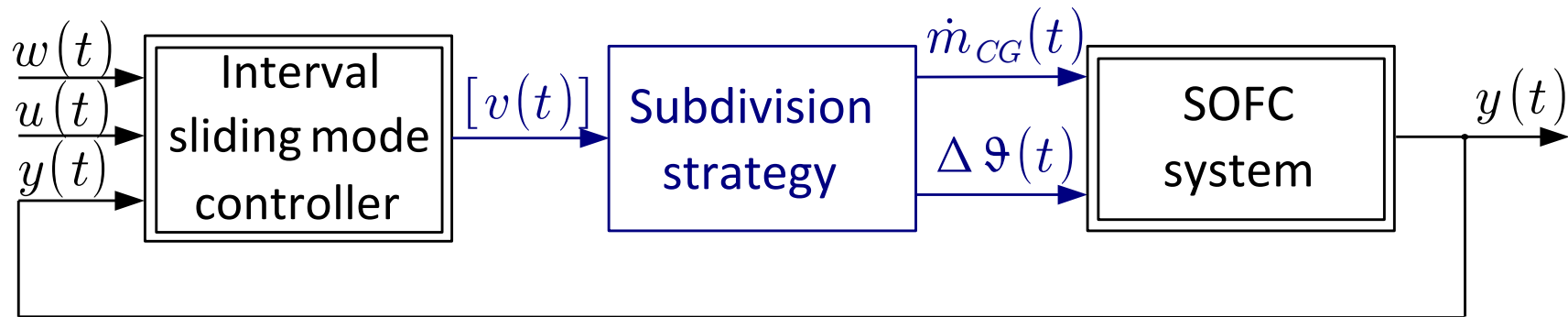
Robust Sliding Mode Control

- Output of exact linearizing feedback control law $u(t)$ with switching to the output of the interval-based sliding mode controller $v(t)$ at the point of time $t = 2.5 \cdot 10^4\text{s}$



Problem: Adequate setting of the SOFC system input $u = \dot{m}_{CG}\Delta\vartheta$ with an available sliding mode controller output $v(t)$

Robust Sliding Mode Control



- Subdivision strategy to determine appropriate control inputs \dot{m}_{CG} and $\Delta\vartheta$ corresponding to $[v(t)]$
- The product of the mass flow \dot{m}_{CG} and of the temperature difference $\Delta\vartheta$ determines the system input

$$u := (\dot{m}_{CG} \cdot \Delta\vartheta)$$

- Operating ranges of the actuators are defined by bounded intervals

Implementation of the Interval-Based Control Law in Simulations

- A **splitting procedure** is employed in each time step k starting with the initial interval box described by $[\dot{m}_{CG}^{<0>}]$ and $[\Delta\vartheta^{<0>}]$ which is identical to the physical actuator constraints
- Multi-sectioning of the input interval vector $[\dot{m}_{CG}^{<l>} ; [\Delta\vartheta^{<l>}]]^T$ into the four interval boxes the mass flow and temperature difference in the time step k

$$[\dot{m}_{CG}^{<l>} ; [\Delta\vartheta^{<l>}]]^T := \begin{bmatrix} [\inf([\dot{m}_{CG}^{<l>}]) ; \text{mid}([\dot{m}_{CG}^{<l>}])] \\ [\inf([\Delta\vartheta^{<l>}]) ; \text{mid}([\Delta\vartheta^{<l>}])] \end{bmatrix}$$

$$[\dot{m}_{CG}^{<L+1>} ; [\Delta\vartheta^{<L+1>}]]^T := \begin{bmatrix} [\text{mid}([\dot{m}_{CG}^{<l>}]) ; \text{sup}([\dot{m}_{CG}^{<l>}])] \\ [\inf([\Delta\vartheta^{<l>}]) ; \text{mid}([\Delta\vartheta^{<l>}])] \end{bmatrix}$$

$$[\dot{m}_{CG}^{<L+2>} ; [\Delta\vartheta^{<L+2>}]]^T := \begin{bmatrix} [\inf([\dot{m}_{CG}^{<l>}]) ; \text{mid}([\dot{m}_{CG}^{<l>}])] \\ [\text{mid}([\Delta\vartheta^{<l>}]) ; \text{sup}([\Delta\vartheta^{<l>}])] \end{bmatrix}$$

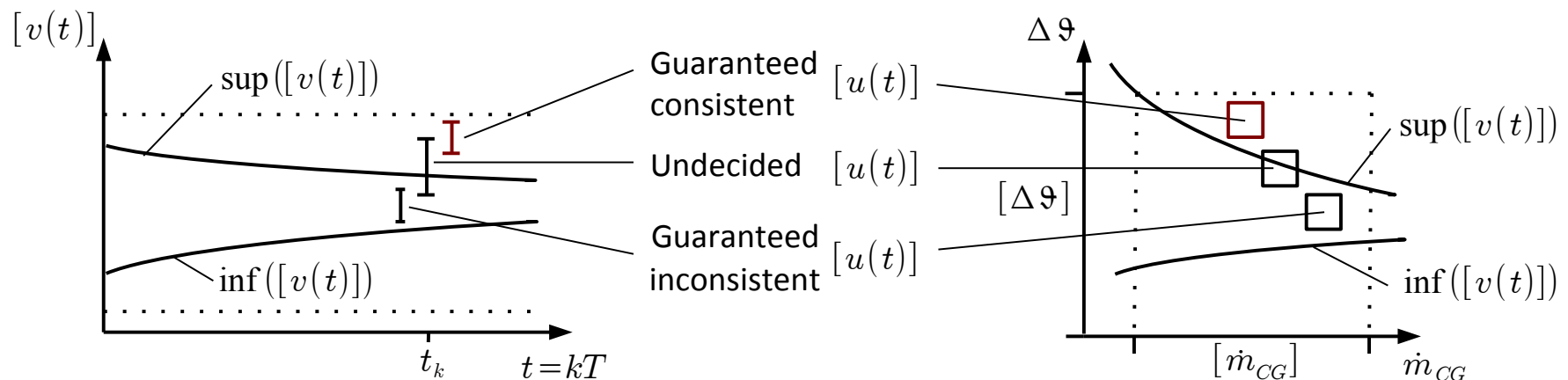
$$[\dot{m}_{CG}^{<L+3>} ; [\Delta\vartheta^{<L+3>}]]^T := \begin{bmatrix} [\text{mid}([\dot{m}_{CG}^{<l>}]) ; \text{sup}([\dot{m}_{CG}^{<l>}])] \\ [\text{mid}([\Delta\vartheta^{<l>}]) ; \text{sup}([\Delta\vartheta^{<l>}])] \end{bmatrix}$$

Implementation of the Interval-Based Control Law in Simulations

- A **validity test** for $[u^{<l>}] = [\dot{m}_{CG}^{<l>}] [\Delta\vartheta^{<l>}]$ is performed according to the controller output $[v]$ to classify **guaranteed consistent**, **undecided**, and **guaranteed inconsistent** input intervals
- Consistency of $[u^{<l>}]$ in $[v]$ (coming directly from the control law) is proven if

$$\sup\{[v]\} < \inf\{[u^{<l>}]\} \text{ for } s \geq 0$$

$$\inf\{[v]\} > \sup\{[u^{<l>}]\} \text{ for } s < 0$$
- Illustration of the consistency test for $s > 0$ with given actuator constraints (dashed lines)



Implementation of the Interval-Based Control Law in Simulations

- Possible compositions of $u(t)$ are assessed for l subintervals in each time step k
- Detection of an optimal interval box for $[\dot{m}_{CG}]$ and $[\Delta\vartheta]$ using the quality criterion

$$[J_k^{<l>}] = \kappa_1 \left([\Delta\vartheta_k^{<l>}] - [\Delta\vartheta_{nom}] \right)^2 + \kappa_2 \left([\Delta\vartheta_k^{<l>}] \right)^2 + \kappa_3 \left([\dot{m}_{CG,k}^{<l>}] - [\dot{m}_{nom}] \right)^2$$

- The minimization of $J_{opt} = \min \left(\inf \left([J_k^{<l>}] \right) \right)$ yields

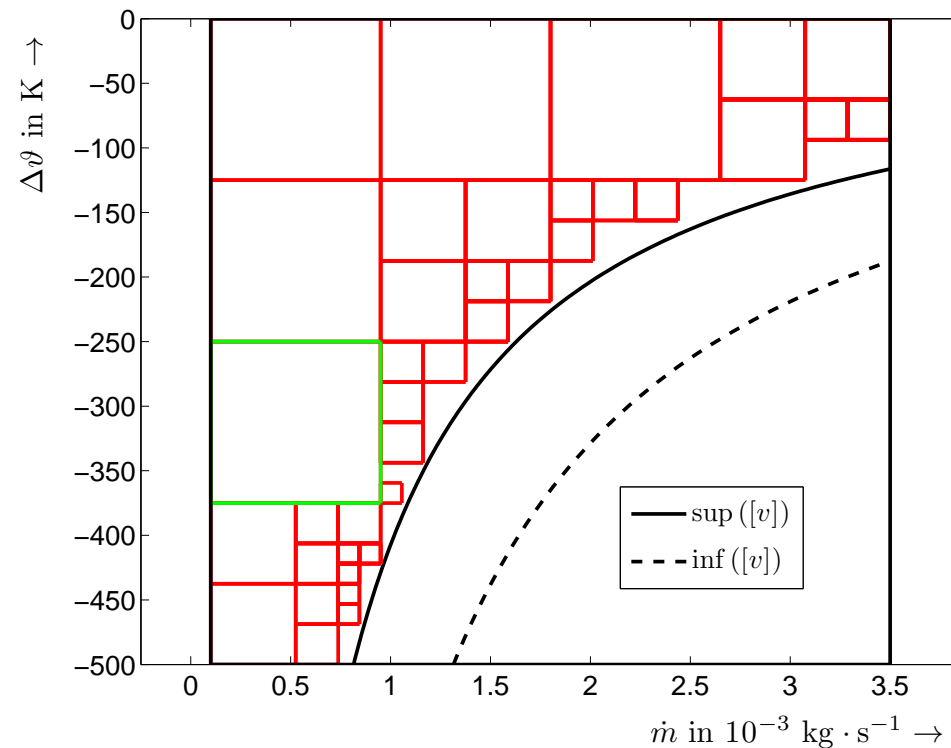
$$[\dot{m}_{CG}^{<opt>}] \quad \text{and} \quad [\Delta\vartheta^{<opt>}]$$

- Definition of the guaranteed stabilizing control signal for the SOFC system with $v \geq \sup([v])$ according to

$$u(t) = \text{mid} \left([\dot{m}_{CG}^{<opt>}] \cdot [\Delta\vartheta^{<opt>}] \right)$$

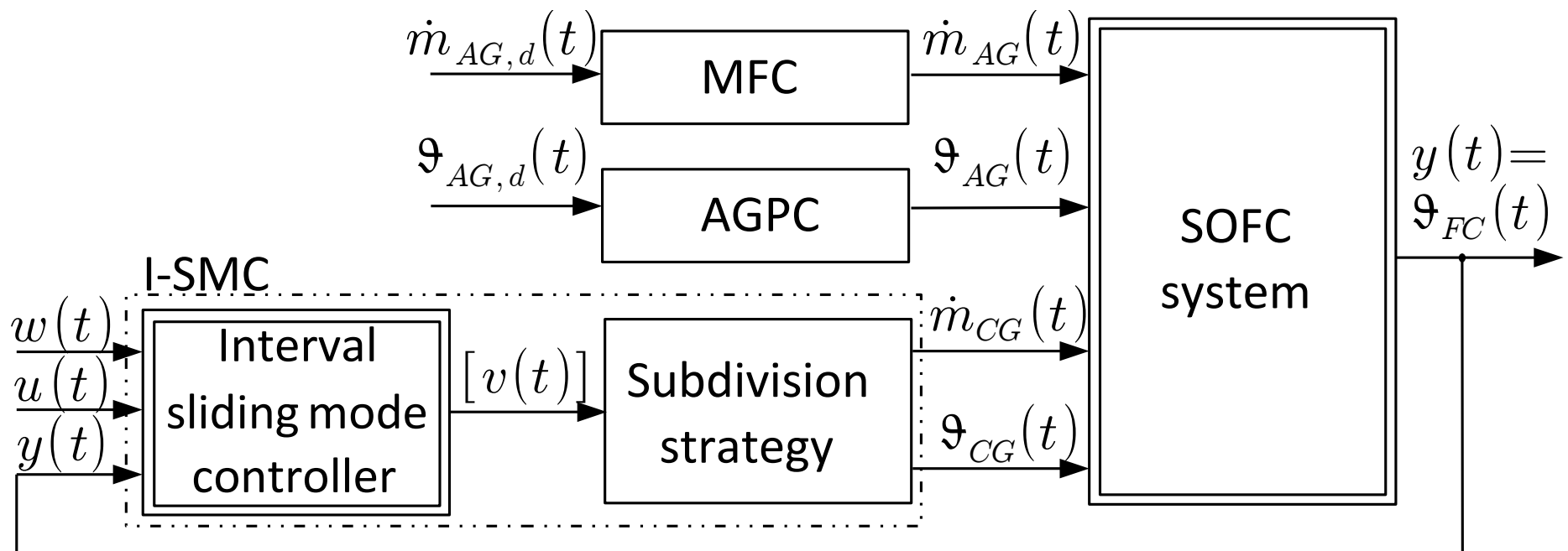
Implementation of the Interval-Based Control Law in Simulations

- Depiction of the optimal system input with nominal values for \dot{m}_{nom} and $\Delta\vartheta_{nom}$
- Cooling process with a value $s > 0$ in the sliding mode control design



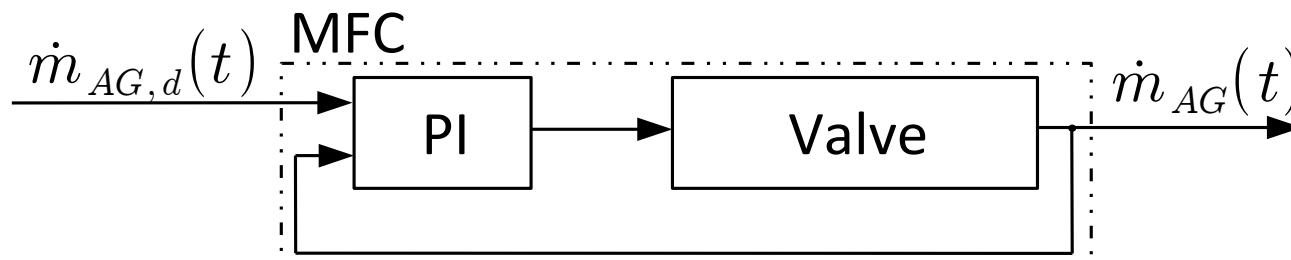
Implementation of the Interval-Based Control Law on the SOFC Test Rig

- Modification of the enthalpy flow of the cathode gas to stabilize a desired operating point
- Optimal choice for \dot{m}_{CG} and ϑ_{CG} to manipulate the enthalpy flow of the cathode gas for an appropriate stabilization of the temperature $y(t) = \vartheta_{FC}$



Implementation of the Interval-Based Control Law on the SOFC Test Rig

- Both the mass flow controller (MFC) and the anode gas preheater controller (AGPC) are used to set up a constant operating point for the anode gas
- Underlying controllers for the cathode gas mass flow (MFC) and the cathode gas preheater temperature (CGPC) are integrated into the structure for the interval-based sliding mode control (I-SMC)
- Example: Block diagram of the underlying PI control for the anode gas mass flow \dot{m}_{AG} through the input valve:



Conclusions and Outlook

Conclusions

- Nonlinear modeling of the thermal subsystem of SOFCs including uncertainty in parameters and system states
- Design of an interval-based sliding mode controller capable of handling bounded uncertainty in a desired operating point
- Optimal adjustment of the enthalpy flow as a control input of the system employing a subdivision strategy regarding actuator constraints
- Real-time capability has been shown by simulations of the interval-based sliding mode control strategy implemented in C-XSC

Dötschel, Thomas; Rauh, Andreas; Aschemann, Harald: *Reliable Control and Disturbance Rejection for the Thermal Behavior of Solid Oxide Fuel Cell Systems*, presented at MATHMOD 2012, Vienna, Austria, 2012. to appear on IFAC-PapersOnLine.net

Conclusions and Outlook

Outlook

- Proof of the robustness in case of switching the output y to other volume elements, where the remaining system dynamics have to be enclosed in state intervals
- Continuation of the experimental validation of the presented approaches for the SOFC system available at the Chair of Mechatronics at the University of Rostock
- Further refinement of the control approach and real-time capable implementation in C-XSC, interfaced with MATLAB, REAL TIME WORKSHOP, LABVIEW, and NATIONAL INSTRUMENTS SIMULATION INTERFACE TOOLKIT
- Further background concerning the control procedure

Rauh, Andreas; Aschemann, Harald: *Interval-Based Sliding Mode Control and State Estimation for Uncertain Systems*, IEEE Intl. Conference on Methods and Models in Automation and Robotics MMAR 2012, Miedzyzdroje, Poland, 2012.

Vielen Dank für Ihre Aufmerksamkeit!

Thank you for your attention!

Merci beaucoup pour votre attention!

Спасибо за Ваше внимание!

Dziękuję bardzo za uwagę!

¡muchas gracias por su atención!

Grazie mille per la vostra attenzione!

